Multivariate biophysical markers predictive of mesenchymal stromal cell multipotency

Wong Cheng Lee[a,b,1], Hui Shi[b,1], Zhiyong Poon[b], Lin Myint Nyan[b], Tanwi Kaushik[c], G. V. Shivashankar[b,d,e], Jerry K. Y. Chan[b,c,f,g], Chwee Teck Lim[a,b,e,h], Jongyoon Han[b,i,j], and Krystyn J. Van Vliet[b,j,k,2]

[a]National University of Singapore Graduate School for Integrative Sciences and Engineering, Singapore 119077; [b]BioSystems and Micromechanics Interdisciplinary Research Group, Singapore-MIT Alliance in Research and Technology, Singapore 138602; [c]Department of Obstetrics and Gynaecology, National University of Singapore, Singapore 119228; [d]Department of Biological Sciences, National University of Singapore, Singapore 117543; [e]Mechanobiology Institute, Singapore 117411; [f]Division of Reproductive Medicine, KK Women's and Children's Hospital, Singapore 229899; [g]Duke-National University of Singapore, Singapore 169857; [h]Department of Biomedical Engineering, National University of Singapore, Singapore 117575; Departments of [i]Electrical Engineering and Computer Science, [j]Biological Engineering, and [k]Materials Science and Engineering, Massachusetts Institute of Technology, Cambridge, MA 02139

Edited by David A. Weitz, Harvard University, Cambridge, MA, and approved September 3, 2014 (received for review February 11, 2014)

The capacity to produce therapeutically relevant quantities of multipotent mesenchymal stromal cells (MSCs) via in vitro culture is a common prerequisite for stem cell-based therapies. Although culture expanded MSCs are widely studied and considered for therapeutic applications, it has remained challenging to identify a unique set of characteristics that enables robust identification and isolation of the multipotent stem cells. New means to describe and separate this rare cell type and its downstream progenitor cells within heterogeneous cell populations will contribute significantly to basic biological understanding and can potentially improve efficacy of stem and progenitor cell-based therapies. Here, we use multivariate biophysical analysis of culture-expanded, bone marrow-derived MSCs, correlating these quantitative measures with biomolecular markers and in vitro and in vivo functionality. We find that, although no single biophysical property robustly predicts stem cell multipotency, there exists a unique and minimal set of three biophysical markers that together are predictive of multipotent subpopulations, in vitro and in vivo. Subpopulations of culture-expanded stromal cells from both adult and fetal bone marrow that exhibit sufficiently small cell diameter, low cell stiffness, and high nuclear membrane fluctuations are highly clonogenic and also exhibit gene, protein, and functional signatures of multipotency. Further, we show that high-throughput inertial microfluidics enables efficient sorting of committed osteoprogenitor cells, as distinct from these mesenchymal stem cells, in adult bone marrow. Together, these results demonstrate novel methods and markers of stemness that facilitate physical isolation, study, and therapeutic use of culture-expanded, stromal cell subpopulations.

mesenchymal stem cell enrichment | biophysical characterization | biomarkers | stem cell heterogeneity | multipotency

The biophysical state of a cell is potentially a rich source of information indicative of cell identity and physiology. When the underlying biochemical activity that occurs as cells replicate, senesce, differentiate, become malignant, or undergo apoptosis is manifest as measurable changes in biophysical characteristics, then parameters such as cell size or mechanical stiffness (1–4) may serve as predictive markers of cellular fate. For example, the metastatic competence of cancer cell lines has been correlated with average mechanical creep compliance (5, 6), and the stiffness of malaria-infected (7) and sickle red blood cells (8) has been related to disease stage and severity.

The successful application of mechanobiology to the analysis of human disease has prompted development of biophysical cytometry methods to study the functional multipotency of stem cells (9, 10). However, such efforts to predict multipotency or "stemness" are challenging due to potential coupling or plurality of biophysical changes in response to distinct cues. For example, changes in cell size are not only related to cell cycle events (11) and cell proliferation rates (12), but also to the reported differentiation capacity of progenitor cells derived from corneal epithelium (13), adipose tissue (14), or adult bone marrow (15, 16). It is thus evident that a more comprehensive physical profile of stem cells is required to consider whether biophysical markers are robust indicators of inducible function in vitro and in vivo. Herein, we demonstrate that multivariate biophysical analysis of cells can readily identify subpopulations of multipotent, as well as osteochondral progenitor, cells within in vitro culture-expanded mesenchymal stromal cells (MSCs).

Although often referred to and treated as a uniform stem cell population, culture-expanded MSCs derived from adult bone marrow (aMSCs) are actually a heterogeneous cell mixture (16, 17). These cell populations exhibit reduced multilineage potential during in vitro culture expansion (18, 19). This decreased multipotency has been attributed to environmental cues (20–25) during in vitro culture and results in MSC subpopulations that render it difficult to study and engineer "stem cell behavior." Such desirable behavior includes self-renewal and multilineage differentiation in vitro or production of uniform, robust therapeutic responses in vivo. However, the long-term and large-scale expansion of aMSCs is necessary to obtain a clinically relevant number of cells for many envisioned tissue regeneration

Significance

We identify a set of unique biophysical markers of multipotent mesenchymal stromal cell populations. Multivariate biophysical analysis of cells from 10 adult and fetal bone marrow donors shows that distinct subpopulations exist within supposed mesenchymal stem cell populations that are otherwise indistinguishable by accepted stem cell marker surface antigens. We find that although no single biophysical parameter is wholly predictive of stem cell multipotency, three of these together—cell diameter, cell mechanical stiffness, and nuclear membrane fluctuations—distinguish multipotent stem cell from osteochondral progenitor subpopulations. Together, these results (along with the corresponding statistical correlations) show that a minimal set of biophysical markers can be used to identify, isolate, and predict the function of stem and progenitor cells within mixed cell populations.

Author contributions: W.C.L., H.S., Z.P., J.H., and K.J.V.V. designed research; W.C.L., H.S., Z.P., L.M.N., and T.K. performed research; L.M.N., G.V.S., J.K.Y.C., and J.H. contributed new reagents/analytic tools; W.C.L., H.S., Z.P., C.T.L., J.H., and K.J.V.V. analyzed data; and W.C.L., H.S., Z.P., and K.J.V.V. wrote the paper.

The authors declare no conflict of interest.

This article is a PNAS Direct Submission.

[1]W.C.L. and H.S. contributed equally to this work.

[2]To whom correspondence should be addressed. Email: krystyn@mit.edu.

This article contains supporting information online at www.pnas.org/lookup/suppl/doi:10.1073/pnas.1402306111/-/DCSupplemental.

therapies. Conventional high-throughput sorting of multipotent MSCs from this heterogeneous, putative MSC population via flow cytometry has proven insufficient, due to the lack of biomolecular surface markers that select specifically for multipotency (15, 26, 27); such molecular labeling approaches also restrict viability and use of such cells for therapeutic applications (28). Thus, it is common to verify the multipotency of MSC subpopulations or clones via in vitro experiments that directly quantify MSC capacity to form colonies and differentiate along multiple tissue lineages. These Schrodinger's cat-like assessments of viable stem cell function are both retrospective and confer obvious limitations for robust studies of stem cell biology and for clinical applications of culture-expanded MSCs. Such considerations illustrate the need for alternative, multivariate, and functional cytometry platforms and methods that can identify marrow stromal cell subpopulations of predictable potency or progenitor status, without labeling or differentiating those cells.

Here, we quantify several biophysical characteristics of MSCs subpopulations derived from human adult and fetal bone marrow. These potential multivariate biomarkers of MSC potency are as follows: (*i*) suspended cell diameter; (*ii*) adherent cell spread area; (*iii*) cell stiffness; (*iv*) nuclear to cytoplasmic ratio; and (*v*) relative nuclear membrane fluctuations. We correlated each property with molecular surface markers, in vitro multilineage differentiation potential, and in vivo regenerative potential (see *SI Appendix* for discussion of previous studies that noted one or more of these properties to be potential indicators of differentiation capacity or commitment). Of particular interest is whether any of these physical signatures, or combinations thereof, could prospectively identify and sort multipotent MSC subpopulations from precommitted progenitor cells. We find that cell size is a necessary but insufficient predictor of MSC multipotency: not all subpopulations of small diameter are multipotent, as might be inferred from previous in vitro studies that compared smaller and larger MSCs (16). Among the several other biophysical markers considered, we find that only cell stiffness and nuclear fluctuations correlated strongly with in vitro differentiation potential and in vivo bone and muscle regeneration capacity. Specifically, adult and fetal MSC subpopulations of sufficiently low mean diameter ($D < 20$ μm), low mechanical stiffness ($E < 375$ Pa), and high nuclear fluctuations ($NF > 1.2\%$) consistently exhibited multipotency in vitro and in vivo. All other MSC subpopulations exhibited commitment toward the osteogenic lineage. Together these findings suggest a minimal set of biophysical markers exist for the identification of MSC and progenitor subpopulations toward clinical applications.

Results

One or multiple biophysical characteristics may serve as a sufficient set to identify stem cells of predictable potency. However, a comprehensive assessment of these potential biophysical markers for prospective in vitro and in vivo outcomes remains lacking. Below, we consider correlations of multipotency with each of these potentical biophysical markers, starting with cell diameter. As human bone marrow-derived MSCs demonstrate differentiation behavior that depends strongly on both culture conditions and donor source (29), we considered 10 donor sources (5 adult donor sources, denoted aD1–aD5, and 5 fetal donor sources, denoted fD1–fD5) under identical in vitro culture conditions.

Size-Based Microfluidic Sorting. aMSCs are known to exhibit heterogeneity in size and loss of multipotency when expanded in culture (30, 31); in contrast, fetal MSCs (fMSCs) remain consistently small in size and are reported to be multipotent even after extended in vitro expansion (32). Thus, given our own observations and previous qualitative reports that smaller aMSCs proliferate more rapidly and appear similar to fMSCs in adherent cell morphology, we first considered whether cell size was strongly correlative with MSC phenotype and differentiation potency. This analysis was enabled by size-based sorting of suspended cells in a microfabricated inertial microfluidic spiral channel device (33) (Fig. 1*A*), into multiple outlet streams (here, outlets 1, 2, 3, and 4) of decreasing cell diameter. This high-throughput sorting system can fractionate up to $>10^7$ cells/h, significantly exceeding that reported previously for other microfluidics-based methods and enabling us to isolate MSC subpopulations with sufficient efficiency, quantity, and cell viability (>90%) (33) required of subsequent biophysical characterization and biochemical assays. This method is detailed in *SI Appendix*.

Table 1 shows the mean suspended cell diameter for size-sorted subpopulations from each donor; from donor aD1, for example, cells collected from outlet 1 were of mean cell diameter $D = 25.5 \pm 0.5$ μm and from outlet 4 were of $D = 17.8 \pm 0.2$ μm. Among all adult donors, MSC subpopulations of largest $\underline{D}$ were consistently collected in outlet 1 (25.7 ± 0.7 μm, termed hereafter as $D^{hi} > 20$ μm) and showed minimal overlap in size with subpopulations of smallest mean cell diameter, which were collected in outlet 4 (16.8 ± 0.3 μm, termed hereafter as D^{lo}). Although the population fraction varied among donors, these subpopulations (outlets 1 and 4) represent ∼15% and ∼20% of the entire unsorted cell population at passage 5 (P5), respectively. The D^{hi} and D^{lo} aMSC subpopulations were used for subsequent experiments for each donor source in this study, and their corresponding unsorted aMSCs from the same donor were used as controls. In contrast, fMSCs exhibited less dispersion in cell diameter (∼16 μm, D^{lo}) and could not be further fractionated into size-based subpopulations. *SI Appendix*, Fig. S1 provides these data graphically and shows visually apparent differences in the adherent cell size for D^{hi} and D^{lo} sorted subpopulations.

Cell Size Is Not Wholly Predictive of Multipotency. To consider whether cell size is a necessary and sufficient biophysical marker of stemness, we first tested the correlation between the suspended cell diameter and in vitro multipotency. Following size-based sorting, cells were adhered to tissue culture polystyrene (TCPS) for 24 h before multilineage differentiation potential (adipo-, osteo-, chondro-, and myogenesis) was assessed via established assays. Differentiation positivity and extent were determined by spectrophotometric quantification of lineage-specific metabolite production toward the adipogenic, osteogenic, or chondrogenic lineages on chemical induction of differentiation in vitro; myogenic differentiation was assessed using immunostaining for desmin-expressing cells. Differentiation was considered to have occurred (i.e., differentiation positivity was noted) for subpopulations that produced metabolites or percentage immunopositive greater than the 90th percentile of the noninduced negative controls (*SI Appendix*, Fig. S2); this provided an objective determination of potency (14) that was independent of the extent of differentiation as discussed further in *SI Appendix*, Fig. S2. *SI Appendix*, Figs. S3 and S4 provide representative images from in vitro differentiation for adult and fetal MSCs, respectively, that were a subset of data in *SI Appendix*, Fig. S2. Subpopulations that showed differentiation toward either three or four of these lineages (adipo-, osteo-, chondro-, and myogenic) were noted as multipotent, whereas subpopulations that exhibited commitment toward either two or one lineage were considered as bipotent and unipotent, respectively. Notably, across all adult and fetal donors screened, bipotent groups were only able to differentiate along both the osteogenic and chondrogenic lineages. No subpopulation was unipotent or showed a total lack of differentiation capacity, in contrast to previous reports of bone marrow-derived MSC clones exhibiting very low prevalence of adipo-chondro, adipo-osteo, and unipotent phenotypes (34); this may be attributed to low prevalence of those phenotypes in nonclonal cultures.

Table 1 illustrates that all aMSC subpopulations of large diameter (D^{hi} aMSCs) were bipotent (osteogenic and chondrogenic),

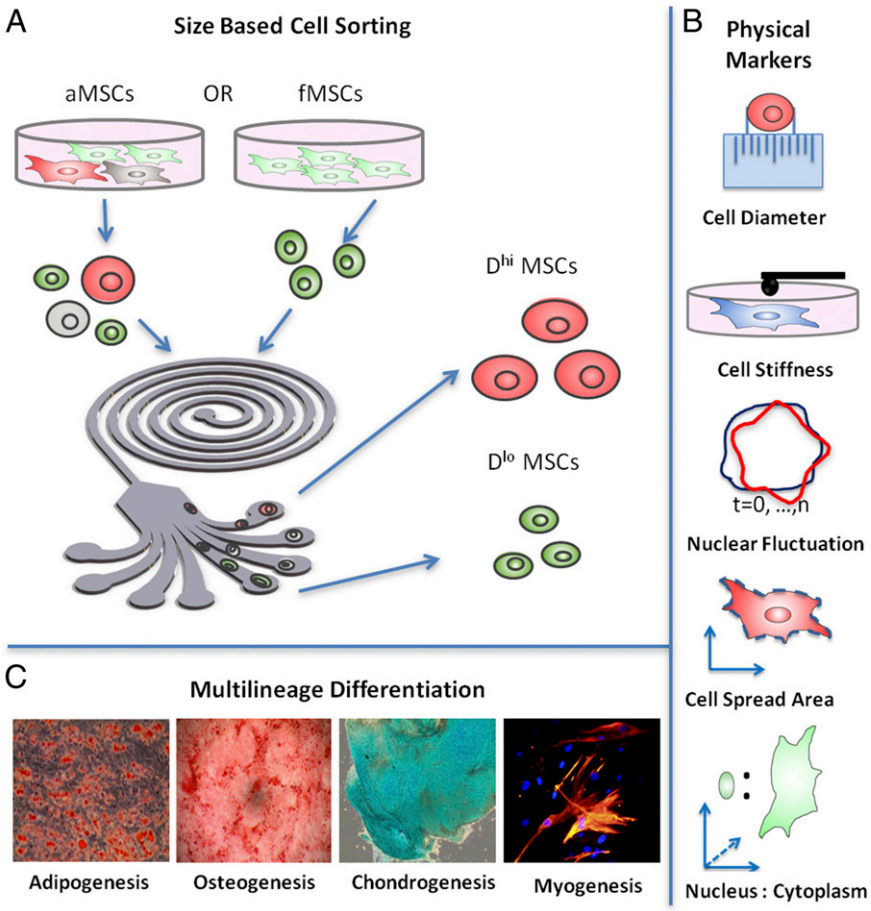

Fig. 1. Schematic of study. (*A*) aMSCs are heterogeneous in size and were first size sorted using a microfabricated spiral microchannel into four fractions (outlets 1, 2, 3, and 4) of decreasing cell diameter. Subpopulations of largest diameter (outlet 1; ~25 μm, D^{hi}) and subpopulations of smallest diameter (outlet 4; ~16 μm, D^{lo}) were used for subsequent experiments for each donor source; the corresponding unsorted aMSCs from the same donor (~21 μm) were used as the control. fMSCs exhibit less dispersion in size (~16 μm, D^{lo}) and could not be further fractionated as a function of diameter. (*B*) After size separation, the D^{lo} and D^{hi} MSC subpopulations were further characterized in terms of cell stiffness, relative nuclear fluctuation, cell spread area, and nucleus-to-cytoplasm ratio. (*C*) Biophysical markers from each MSC subpopulation were then correlated with in vitro differentiation capacity along four lineages: fat, bone, cartilage, and muscle, and also with in vivo bone growth and muscle repair summarized in Fig. 5.

three of the five small-diameter subpopulations (D^{lo} aMSCs) were multipotent, and three of the five fMSC donors were multipotent. The relative potency of D^{hi} vs. D^{lo} subpopulations for aMSCs and for fMSCs was consistent at different cell passage numbers (population doublings), as tabulated in *SI Appendix*, Table S1 for both passages 5 and 8 (see *SI Appendix*, Tables S1 and S2 for data and discussion of how shifts in subpopulation prevalence can change the apparent potency of an unsorted MSC population over multiple passages). Spearman's correlation analysis was used to determine the strength and significance level of correlation between the potency and mean cell diameter of each subpopulation of MSCs. The correlation between cell size and multipotency was not strong ($r = -0.551$, $P = 0.033$; *Methods* and *SI Appendix*, Table S3). Thus, as cell size alone was an insufficient biophysical predictor of multipotency, we next considered whether one or more other properties (cell stiffness, nuclear fluctuations, cell spread area, and relative nuclear-to-cytoplasm ratio) would together define the multipotent MSC subpopulations.

Cell Stiffness and Nuclear Membrane Fluctuations Correlate with Multipotency. fMSCs and size-sorted aMSC subpopulations were seeded onto tissue culture polystyrene and allowed to attach and spread before subsequent characterization of mechanical stiffness E and nuclear fluctuations NF. Physical sorting into D^{hi} and D^{lo} subpopulations did not detectably alter these properties and was used because this significantly increased the efficiency of these next biophysical, in vitro, and in vivo assays of each subpopulation defined in part by cell diameter. *SI Appendix*, Fig. S5 shows that distributions of measured D, E, and NF were similar, with and without passage of cells through the microfluidic device.

We characterized the mechanical response of attached cells via atomic force microscopy-enabled nanoindentation of the cell body. These measurements provide an effective Young's elastic modulus E of the cell (*Methods* and *SI Appendix*, Fig. S9), and we refer to this quantity as cell stiffness. Mean stiffness E is reported in Fig. 2 as probability distributions, constructed using statistical bootstrapping from 30 to 60 replicate measurements (i.e., cells) for each donor and each subpopulation (35) (*Methods*). Fig. 2 *A* and *B* shows the cell stiffness profile of the D^{hi} aMSCs, D^{lo} aMSCs, and fMSCs from all donor samples. On the high end of the spectrum, the mean stiffness of D^{hi} aMSCs ranged from 460.3 ± 31.0 to 1,100 ± 99.6 Pa among five donors as shown in Table 1 (mean ± SEM). These larger cells were significantly stiffer than the D^{lo} aMSCs (E = 329.6 ± 43.8 Pa for the same five donors) and fMSCs (E = 321.3 ± 31.4 Pa for five donors). Subsequent correlation analyses showed that cell stiffness varied negatively with cell potency ($r = -0.787$, $P < 0.01$;

Table 1. Biophysical markers from different subpopulations of MSCs

Cell population	*D* (μm)	*E* (Pa)	*NF* (%)	*N:C*	*A* (μm^2)	Potency
aD1 O1	25.5 ± 0.5	813.85 ± 64.72	0.94 ± 0.04	0.017 ± 0.001	12,227 ± 760	Bipotent
aD2 O1	24.6 ± 0.4	460.3 ± 31.00	1.02 ± 0.06	0.024 ± 0.001	11,059 ± 468	Bipotent
aD3 O1	26.7 ± 0.3	705.69 ± 76.65	0.96 ± 0.05	0.021 ± 0.001	7,574 ± 335	Bipotent
aD4 O1	24.1 ± 0.4	1100.31 ± 99.57	1.09 ± 0.06	0.047 ± 0.002	5,315 ± 207	Bipotent
aD5 O1	27.7 ± 0.4	543.84 ± 30.92	0.94 ± 0.05	0.026 ± 0.001	8,213 ± 213	Bipotent
aD1 O4	17.8 ± 0.2	274.88 ± 19.32	1.25 ± 0.07	0.036 ± 0.002	4,098 ± 178	Multipotent
aD2 O4	14.5 ± 0.2	220 ± 20.29	1.43 ± 0.05	0.054 ± 0.002	3,675 ± 96	Multipotent
aD3 O4	16.7 ± 0.2	340.05 ± 28.75	1.37 ± 0.07	0.042 ± 0.001	2,988 ± 80	Multipotent
aD4 O4	17.1 ± 0.2	508.86 ± 33.02	1.31 ± 0.08	0.090 ± 0.002	2,015 ± 50	Bipotent
aD5 O4	17.8 ± 0.2	304.55 ± 25.34	1.13 ± 0.07	0.058 ± 0.001	3,051 ± 54	Bipotent
fD1	16.0 ± 0.2	291.43 ± 18.63	1.34 ± 0.10	0.071 ± 0.002	3,242 ± 137	Multipotent
fD2	17.2 ± 0.1	210.96 ± 14.00	1.42 ± 0.08	0.054 ± 0.004	2,466 ± 122	Multipotent
fD3	16.9 ± 0.1	338.32 ± 16.95	1.42 ± 0.05	0.043 ± 0.003	1,729 ± 182	Multipotent
fD4	17.0 ± 0.3	425.46 ± 26.33	1.20 ± 0.05	0.071 ± 0.005	2,479 ± 88	Bipotent
fD5	17.1 ± 0.3	340.51 ± 22.36	1.06 ± 0.05	0.102 ± 0.01	1,537 ± 90	Bipotent

D (suspended cell diameter), *E* (effective cell elastic modulus), *NF* (relative nuclear fluctuations), *N:C* (nuclear to cytoplasmic ratio), and *A* (attached cell spread area). Data are presented as mean ± SEM for passage 5. Corresponding population potency of biophysical triplets described by *D*, *E*, and *NF* is also indicated in green (multipotent: adipo-, osteo-, chondro-, and myogenic,) or red (bipotent: osteo-, chondrogenic), respectively. Mean *D*, *E*, and *NF* corresponding to values below (for *D* and *E*) and above (for *NF*) bipotency thresholds discussed in the text are indicated in green and otherwise are red.

SI Appendix, Table S3). Specifically, we observed that MSCs from both adult and fetal sources that exhibited $E > 375$ Pa also exhibited osteochondral biopotency, regardless of whether these stiffer groups were categorized as D^{lo} or D^{hi} subpopulations. *SI Appendix*, Fig. S5*B* shows that *E* of these subpopulations was not detectably altered by first sorting subpopulations by cell diameter.

This observation that stiffer, uninduced MSCs exhibit limited potency and osteogenic commitment is consistent with other related works that showed the tendency of attached and undifferentiated stem cells to become stiffer during differentiation (36) or in comparison with osteoblasts (23). For example, Gonzalez-Cruz et al. recently demonstrated positive correlation between stiffness of at-

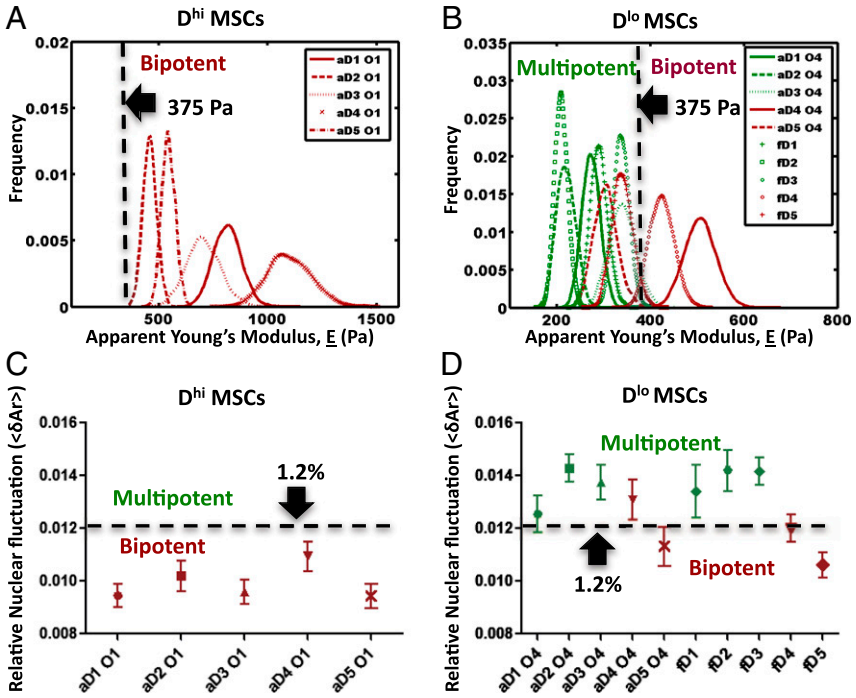

Fig. 2. Cell stiffness and relative nuclear fluctuation correlate with potency of putative MSCs. Thresholds of effective mean elastic modulus *E* and average nuclear fluctuations *NF* were determined experimentally by comparing these mechanical properties of all donor subpopulations sampled against the in vitro multilineage differentiation potential. Multipotent MSC subpopulations exhibited a consistent biophysical phenotype: sufficiently low cell diameter (50), low mechanical stiffness (E^{lo}), and high relative nuclear fluctuation (NF^{hi}) (color-coded green). In contrast, subpopulations that did not meet this criterion (i.e., those that were either large or of high mechanical stiffness or of low relative nuclear fluctuation) were only bipotent (color-coded red). (*A*) Large or D^{hi} MSCs from all adult donors were bipotent and exhibited an average $E > 375$ Pa. (*B*) Similarly, small or D^{lo} MSCs of $E > 375$ Pa (aD4 and fD4) were also bipotent. In contrast, multipotent D^{lo} MSCs were consistently more compliant with $E < 375$ Pa. (*C*) D^{hi} MSCs from all adult donors exhibited an average *NF* of <1.2%, which is in contrast to the (*D*) multipotent D^{lo} MSCs that typically exhibited $NF > 1.2\%$. Notably, D^{lo} MSCs that were bipotent (aD5 and fD5) also exhibited *NF* <1.2%, suggesting that among the many biophysical parameters considered herein, multipotency is characterized minimally by three biophysical criteria ($D^{lo}E^{lo}NF^{hi}$).

tached, adipose-derived stem cells (n = 19–25 cells from 32 clones) and in vitro osteogenic differentiation (14). Although there is a clear link between cell stiffness and osteogenicity, we found that not all mechanically compliant subpopulations with E < 375 Pa were multipotent: aD5 D^{lo} and fD5 D^{lo} donor cells were strongly osteogenic in terms of relative extent of bone mineral production (*SI Appendix*, Figs. S2–S4 for comparisons of alizarin red intensity). This finding indicates that, like cell diameter, cell stiffness alone is also not wholly predictive of stem cell multipotency, and motivates a threshold stiffness of attached MSCs beyond which robust multipotency is not expected. Thus far in our consideration of biophysical markers, the above results show that D^{hi} MSC subpopulations are consistently stiff and bipotent, and D^{lo} MSC subpopulations are either stiff and bipotent or compliant and multipotent.

We next considered whether functional differences among the D^{hi} and D^{lo} subpopulations of MSCs could be correlated with physical fluctuations of the nuclear lamin scaffold. This candidate biophysical marker is motivated by analyses of mouse embryonic stem cells (ESCs), which Bhattacharya et al. showed to exhibit greater nuclear fluctuations than mouse embryonic fibroblasts; this increased nuclear membrane fluctuation or "nuclear fluidity" has been related to the extent and rate of chromatin rearrangement within the nucleus (37). In the present study, MSCs from each donor were size sorted and adhered for 12 h before transfection with EGFP-tagged nuclear membrane protein lamin B1 (EGFP-LaminB1) and subsequent analysis via time-lapsed confocal microscopy (*Methods*). The relative nuclear fluctuations were quantified in terms of changes in the projected nuclear area ($<\delta Ar \geq \sum \delta Ar_i/n$) over all time points (7 min) as a measure of relative nuclear fluidity (see *Methods* and *SI Appendix*, Fig. S10 for calculation details). Larger or D^{hi}MSCs generally exhibited lower relative nuclear fluctuation NF (0.90 ± 0.02% to 1.12 ± 0.02%, mean ± SEM), whereas D^{lo}MSCs from adult or fetal donors tended to exhibit higher NF as shown in Table 1 (and *SI Appendix*, Table S1). *SI Appendix*, Fig. S5*C* shows that NF of these subpopulations was not detectably altered by first sorting subpopulations by cell diameter.

Correlation analyses revealed that MSC potency was generally correlated positively with NF (r = 0.852, P < 0.05; *SI Appendix*, Table S3), independently of cell diameter. As in the case of cell stiffness, threshold segmentation was observed to be able to distinguish multipotent and progenitor subpopulations: Fig. 2 *C* and *D* shows that subpopulations of lower NF (<1.2%) were bipotent and exhibited only osteo-chondrogenic differentiation potential. Note that this observation of the restricted potencies in subpopulations of low NF included those of small cell diameter (D^{lo} aD5 and fD5), which were not predicted previously by cell stiffness measurements. However, considerations of the NF magnitude alone were also not wholly predictive of multipotency for MSCs exhibiting higher NF (>1.2%). In fact, D^{lo} aD4 and fD4 subpopulations were bipotent and exhibited high NF; however, these MSCs also exhibited cell stiffness exceeding the threshold E of ∼375 Pa that correlated with bipotent D^{hi} MSCs subpopulations. These findings in human MSCs are consistent with recent studies (37, 38) that demonstrated that terminally differentiated primary mouse embryonic fibroblasts exhibit less dynamic nuclear organization than undifferentiated mouse ESCs; those nuclear area fluctuations correlated with higher chromatin dynamics (38). These higher fluctuations of chromatin and nuclear area NF in the stem cell nuclei are interpreted as a functional capacity of chromosomes to reconfigure in the undifferentiated state (39).

Thus, in our consideration of these three candidate biophysical markers, none can singly be wholly predictive of multipotency. However, we found that cell populations that are small and mechanically compliant and exhibit higher nuclear membrane fluctuations are also consistently multipotent. Next, let us consider two additional candidate markers of multipotency, also motivated by qualitative analogy to pluripotent ESCs.

Cell Spread Area and Nucleus:Cytoplasm Ratio Do Not Correlate with Multipotency. The projected contact area between cells and tissue culture polystyrene (i.e., cell spread area A), as well as the volumetric ratio of the cell nucleus to cytoplasm ($N{:}C$), of adherent MSCs was measured via fluorescence staining and confocal analysis. We identified no detectable correlation (*SI Appendix*, Table S3) between attached cell spread area and potency state (r = −0.134, P > 0.1) or between $N{:}C$ ratio and potency state (r = −0.245, P > 0.1) in MSCs. We note that others have observed that the $N{:}C$ ratios of undifferentiated ESCs decrease significantly during lineage commitment (40) and that correlation exists between $N{:}C$ and stiffness/multipotency of suspended stem cells (41). In our studies, we intentionally maintained subconfluent cell cultures as discussed by Sekiya et al. (29) to minimize the uncharacteristically increased cell spreading as cells approach confluency.

A Minimal Set of Biophysical Markers of Stem Cell Multipotency. Overall, these findings suggest the need for multivariate biophysical characterization, as is also often required for robust biomolecular characterization of phenotype via antigen labeling. These results reveal a minimal set of biophysical markers that are indicative of a cell subpopulation's differentiation potency: cell diameter D, cell stiffness E, and relative nuclear fluctuations NF. To consider and denote this, we assigned fixed thresholds of each parameter to describe subpopulations of MSCs in biophysical marker categories, reminiscent of relative expression levels of biochemical markers of phenotype. The four resulting categories of putative MSCs are $D^{lo}E^{lo}NF^{hi}$, $D^{lo}E^{lo}NF^{lo}$, $D^{lo}E^{hi}NF^{hi}$, and $D^{hi}E^{hi}NF^{lo}$ (Fig. 3 *A*–*P*). *SI Appendix*, Table S4 quantifies the percentage difference in D, E and NF subpopulations from the same donor source; on average, for a given donor the larger (D^{hi}) subpopulations were of 60% greater diameter, 150% higher stiffness, and 25% lower nuclear fluctuations. Only culture-expanded subpopulations of small diameter (D < 18 μm) that were also compliant (E < 375 Pa) and exhibited highly dynamic nuclear lamina fluctuations (NF > 1.2%) were multipotent in vitro; the biophysical description of these multipotent MSC subpopulations is that they are $D^{lo}E^{lo}NF^{hi}$ cells. All other categories (cell subpopulations of sufficiently large diameter and/or of sufficiently high stiffness or low nuclear fluctuations) were restricted in potency to osteogenic and chondrogenic lineages and were thus committed osteochondral progenitors (see *SI Appendix*, Table S1 and Figs. S6 and S7 for the corresponding 3D graphical depiction and property distributions of this multivariate characterization of each subpopulation, respectively, and also *SI Appendix, Discussion* for correlations between cell diameter and the extent of osteogenic commitment as quantified by metabolite production).

To further define the functional properties of stemness of each category of MSCs, cells from each subpopulation were seeded via limiting dilution into 96-well plates at one cell per well (n = 3 replicate experiments). Fig. 3*Q* shows that $D^{lo}E^{lo}NF^{hi}$ subpopulations exhibited significantly more colony formation units (CFUs) at 52 ± 3.2% compared with the other three MSC subpopulation categories (P < 0.05). These subpopulations also exhibited a higher proliferation rate (Fig. 3*R*); see *SI Appendix*, Fig. S11 for all donor sets. Our findings detailed in the discussion below further indicate that this biophysical subpopulation description is a necessary and sufficient (compared with the larger set of potential biophysical markers we considered) set of markers that we found to correlate with MSC subpopulation multipotency, genetically, and in vitro and in vivo.

We also note that this minimal set of biophysical markers does not obviate the existence of additional biophysical markers of stemness beyond the many analyzed here. This minimal biophysical

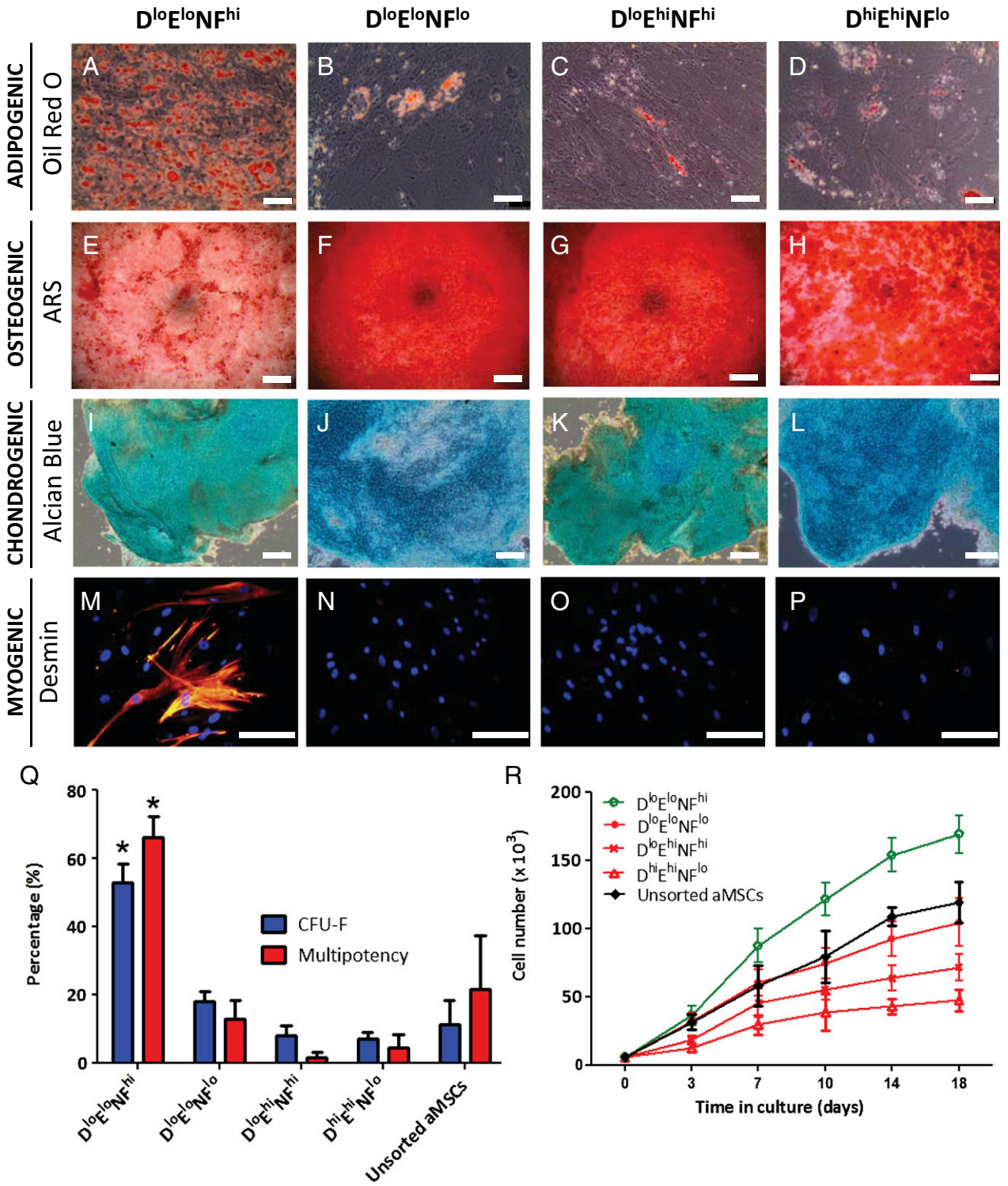

Fig. 3. Multilineage differentiation of MSC subpopulations along (*A–D*) fat, (*E–H*) bone, (*I–L*) cartilage, and (*M–P*) muscle lineages in vitro. Only $D^{lo}E^{lo}NF^{hi}$ MSCs were multipotent (>60%) and consistently exhibited differentiation along all four lineages (*Q*), whereas MSCs that exhibited either high stiffness (51) or low nuclear fluctuation (NF^{lo}) were limited to differentiation along only the osteogenic and chondrogenic lineages. (Scale bar, 50 μm.) The $D^{lo}E^{lo}NF^{hi}$ MSCs also showed higher colony formation efficiency, CFU-F (*Q*), and higher proliferation rate (*R*).

marker set also does not obviate the potential for new biochemical or biomolecular markers, including expression levels of known or yet unidentified cell surface proteins or intracellular macromolecules that may also correlate strongly with this set of biophysical markers of MSC multipotency. Importantly, however, the current set of biomolecular markers that are often used to test for stem cell enrichment do not distinguish among these subpopulations that exhibit clear biophysical and functional differences. *SI Appendix*, Fig. S8 shows that at least these frequently used biomolecular markers failed to resolve differences by

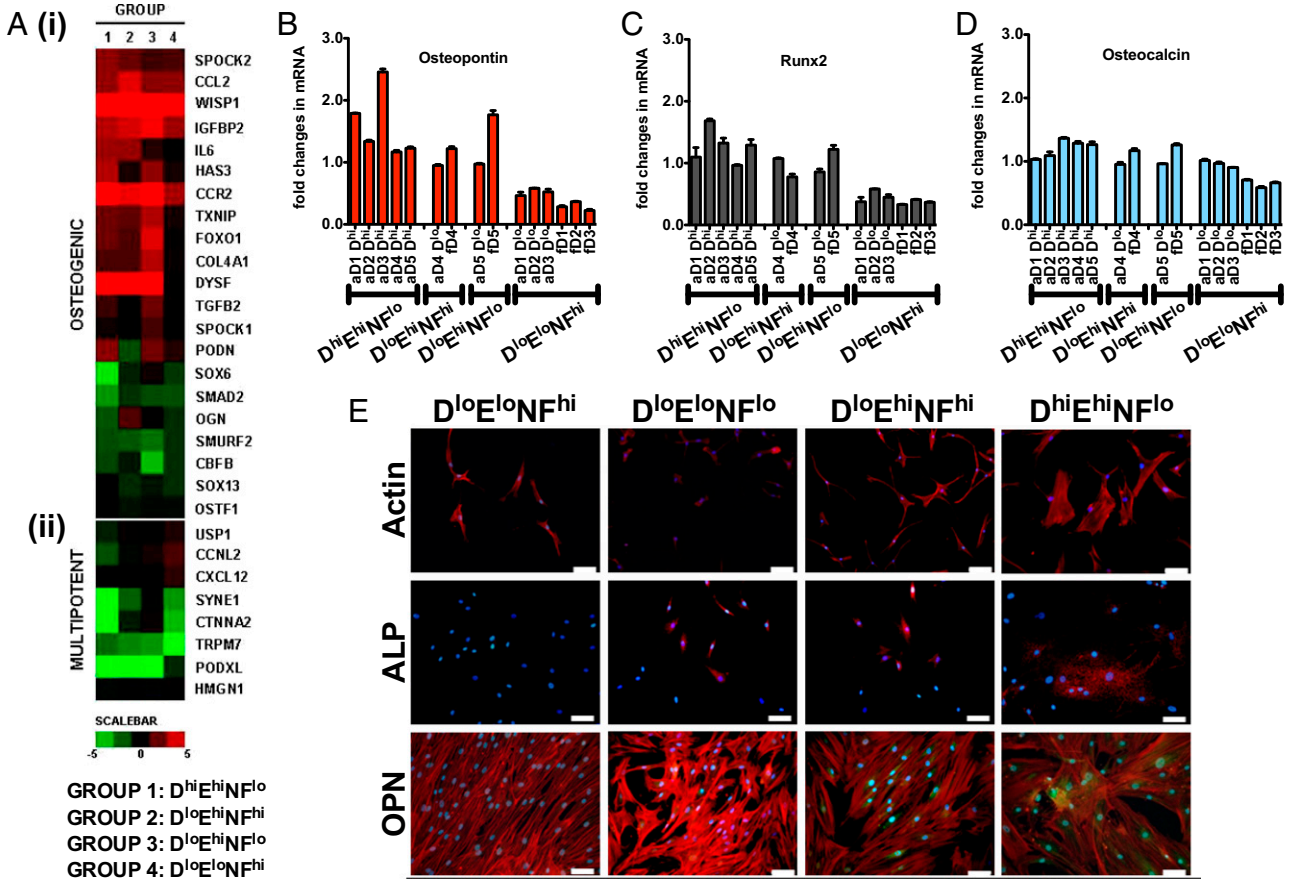

Fig. 4. Microarray heat map of relevant transcripts from a pool of >48,000 human transcripts on the Illumina HT-12 chip, showing differential expression of osteogenic genes (*A, i*), as well as genes associated with maintenance of a stem cell program in MSCs (*A, ii*). These data demonstrate that biophysical cell characterization is an effective means to prospectively identify MSCs that have different levels of lineage commitment. Comparative RT-PCR analysis of the osteogenic gene markers: osteopontin (*B*), runx2 (*C*), and osteocalcin (*D*) in all MSC groups used in the study, normalized by the housekeeping gene GADPH. Significant up-regulation of these important osteogenic markers in the $D^{hi}E^{hi}NF^{lo}$ further confirms that this is a subpopulation of osteogenically committed cells. Immunofluorescent staining of early osteogenic markers, (*E*) alkaline phosphatase (ALP, red) and osteopontin (OPN, green), of MSC subpopulations classified under four categories of cell size, stiffness, and nuclear fluctuations as discussed in the text. A representative subpopulation from each category is shown. All but the $D^{lo}E^{lo}NF^{hi}$ groups show elevated levels of ALP and OPN, indicating that those subpopulations that are not described as $D^{lo}E^{lo}NF^{hi}$ exhibit some level of commitment toward the osteogenic lineage. (Scale bar, 100 μm.)

immunophenotyping among subpopulations that differed in biophysical characteristics and in differentiation potency: MSC subpopulations from all donor sources, both adult and fetal, exhibited a consistent molecular surface marker phenotype that was negative for endothelial (CD31) and hematopoietic (C34 and CD45) markers and positive for putative mesenchymal marker [CD105 (SH2)], and cell adhesion molecules (CD90 and CD106).

Correlation of Cell Biophysical Markers with Gene Transcription and Translation. To determine whether significant genetic differences existed among these subpopulations and might be relevant to the state of differentiation potency, we next compared the transcriptional profile of the MSC subpopulations classified by biophysical markers. Fig. 4 *A, i* shows the heat map of a candidate set of genes generated via microarray analysis. Notable expression of genes such as CCL2, CCR2, IGFBP2, FOXO1, and SPOCK2 indicated osteogenic cell characteristics in the $D^{hi}E^{hi}NF^{lo}$ subpopulation; this finding is consistent with our observations in functional differentiation assays and provides genetic evidence that $D^{hi}E^{hi}NF^{lo}$ cells are osteogenically committed. For cell populations characterized as $D^{lo}E^{lo}NF^{hi}$, no evidence of lineage commitment was evident from microarray analysis. However, cross-referencing of data sets among MSC groups identified a set of up-regulated transcripts (Fig. 4 *A, ii*) that were correlated inversely with those of $D^{hi}E^{hi}NF^{lo}$ subpopulations. Four of these genes (USP1, CCNL2, CXCL12, and PODXL) have been implicated previously as important in the preservation of stem cell fate, as well as in the maintenance of chromosomal structure and activity (30, 42, 43). Although beyond the scope of the present study to fully explore the role of these genes in the multipotency of MSCs, the relative up-regulation of these genes in only the $D^{lo}E^{lo}NF^{hi}$ subpopulation is consistent with the concept that this subpopulation is not lineage committed.

To verify that these biophysical markers also reliably categorized the MSCs at the level of protein expression, we additionally performed RT-PCR and immunocytochemistry. Transcripts for proteins correlative with osteogenic differentiation (osteopontin, Runx2, and late-stage marker ostocalcin) were expressed differentially via RT-PCR (Fig. 4 *B–D*) and were most significantly up-regulated in the $D^{hi}E^{hi}NF^{lo}$ group and down-regulated in the $D^{lo}E^{lo}NF^{hi}$ group. Further, osteopontin and alkaline phosphatase were expressed differentially via immunocytochemical staining (Fig. 4*E*). These findings are consistent with groupings classified by biophysical markers. Specifically, only the $D^{lo}E^{lo}NF^{hi}$ MSCs (from both fetal and adult marrow sources) exhibited protein expression consistent with in vitro differentiation toward all three mesenchymal lineages, whereas the other subpopulations showed decreased adipogenesis and enhanced osteogenic

differentiation potential. Further, the overall gene expression pattern among the different MSC groups also demonstrates that biophysical characterization of these cell populations is efficient for prospectively determining the state of MSC subpopulation differentiation potency.

Biophysical Markers Are Also Predictive of in Vivo End Points. After verifying that the set of biophysical markers allowed characterization of culture-expanded MSCs into different cell subpopulations that exhibit a greater degree of functional homogeneity, we sought to determine whether MSC subpopulations characterized in this manner would result in more potent and reproducible therapeutic effects in vivo. First, to evaluate whether these biophysical markers can identify a particular subpopulation among putative MSCs that exhibits a higher potential for bone tissue engineering applications (44), we seeded each porous osteoinductive polymer scaffold [polycaprolactone-tricalcium phosphate (PCL-TCP) cubes of 5-mm edge length] with a cell subpopulation (or unsorted cells, as

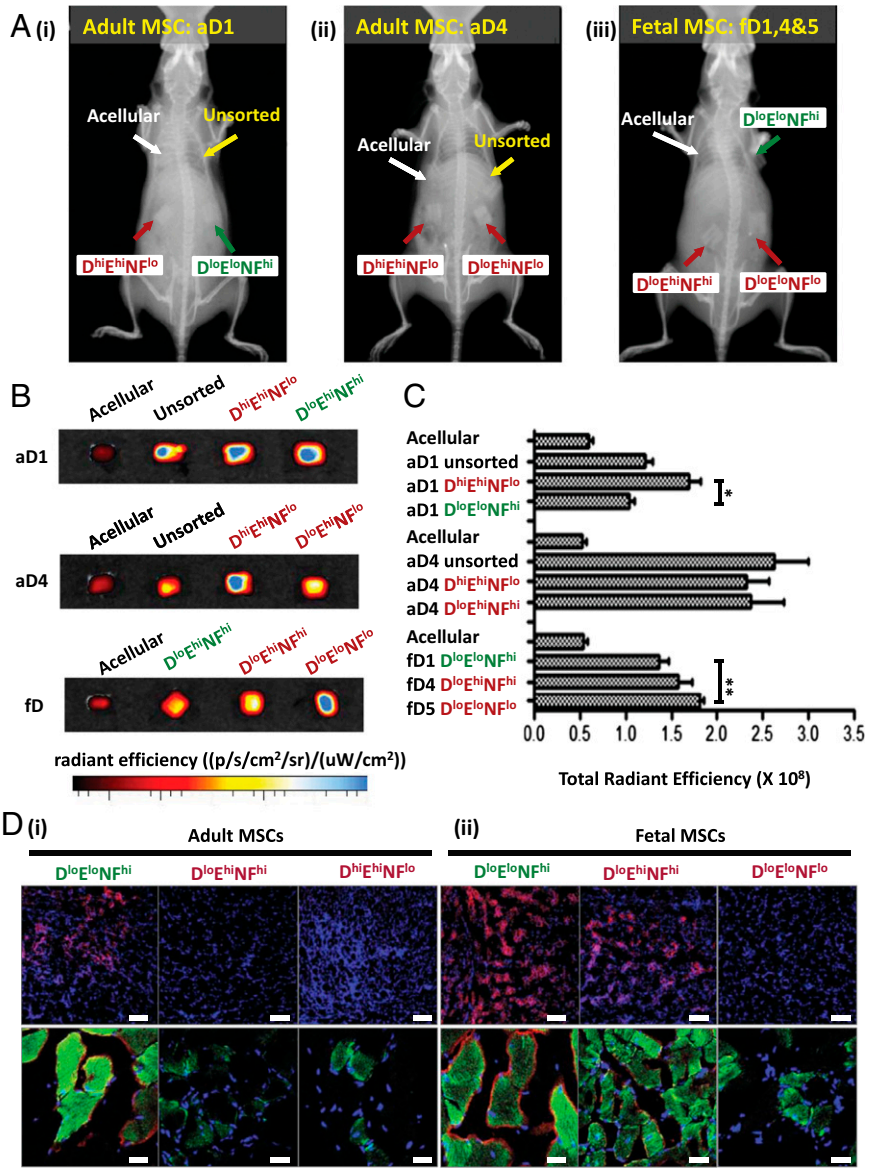

Fig. 5. (*A–C*) In vivo ectopic bone formation of the MSC biophysical categories within PCL-TCP scaffold constructs. Subpopulations from representative cell donor sources are shown. (*A*) Representative X-ray images showing greater contrasts in scaffolds loaded with committed subpopulations (red) of MSCs: (*A, i*) $D^{hi}E^{hi}NF^{lo}$, (*A, ii*) $D^{lo}E^{hi}NF^{hi}$, and (*A, iii*) $D^{lo}E^{lo}NF^{lo}$ compared with the uncommitted $D^{lo}E^{lo}NF^{hi}$ MSCs (green). (*B*) Bone constructs extracted 4 wk after implantation showed that the $E^{lo}NF^{hi}$ MSCs (both adult and fetal) accumulated the least osteosense fluorescent signal ($^*P < 0.05$, two tailed) than the committed subpopulations of MSCs (adult, $P = 0.0048$; fetal, $P = 0.011$), indicating a slower rate of osteogenesis in vivo. (*C*) Osteosense signal quantification revealed enhanced mineralization in the committed subpopulations of MSCs ($D^{hi}E^{hi}NF^{lo}$, $D^{lo}E^{hi}NF^{hi}$, and $D^{lo}E^{lo}NF^{lo}$) compared with the uncommitted $D^{lo}E^{lo}NF^{hi}$ MSCs groups from both adult and fetal donors. (*D*) In vivo myogenic differentiation potential of the different categories of MSCs. Subpopulations from representative cell donor sources are shown. (*D, i*) Immunofluorescent staining of sectioned cardiotoxin-damaged skeletal muscle tissue, 3 wk after infusion with different MSC populations, showed greater engraftment (green) and spectrin formation (red) for the $D^{lo}E^{lo}NF^{hi}$ MSCs. (*D, ii*) Similarly, greater engraftment and spectrin formation was also observed in the $D^{lo}E^{lo}NF^{hi}$ groups in fetal MSCs (Table 1). (Scale bar: 10×, 100 μm; 20×, 50 μm.) Biophysical markers from different subpopulations of MSCs. *D* (suspended cell diameter), *E* (effective cell elastic modulus), and *NF* (relative nuclear fluctuations). Corresponding population potency of biophysical triplets described by *D*, *E*, and *NF* is also indicated in green (multipotent: adipo-, osteo-, chondro- and myogenic,) or red (bipotent: osteo-, chondrogenic), respectively.

indicated) obtained from a single donor source. For example, a scaffold seeded with aD1 $D^{hi}E^{hi}NF^{lo}$ cells comprised the size-sorted subpopulation of larger cells from that donor source, and those larger cells were also stiffer and of lower nuclear fluctuations. All donor sets were included, and this represented all four biophysically distinct groups characterized by combinations of size, stiffness, and nuclear fluctuations ($D^{lo}E^{lo}NF^{hi}$, $D^{lo}E^{lo}NF^{lo}$, $D^{lo}E^{hi}NF^{hi}$, and $D^{hi}E^{hi}NF^{lo}$), as well as nonseeded control scaffolds (*Methods*). These scaffolds were implanted subcutaneously in the dorsum of a single nonirradiated NOD/SCID mouse, and acellular PCL-TCP scaffolds were implanted as a control with $n = 5$ mice per cell donor source and corresponding subpopulation (44). The degree of ectopic bone mineralization on the implanted constructs was evaluated and quantified 4 wk after implantation using X-ray imaging and a systemically injected hydroxyapatite-directed bone-imaging probe (OsteoSense). X-ray imaging showed that the scaffolds containing committed MSC groups ($D^{lo}E^{lo}NF^{lo}$, $D^{lo}E^{hi}NF^{hi}$, and $D^{hi}E^{hi}NF^{lo}$) exhibited a greater extent of bone mineralization compared with the uncommitted $D^{lo}E^{lo}NF^{hi}$ phenotype (Fig. 5*A*). These observations were further confirmed by quantification of the accumulated osteosense fluorescent signal from the implanted scaffolds (Fig. 5 *B* and *C* and *SI Appendix*, Fig. S12 for all donors) and demonstrate that the subpopulations that are determined to be osteoprogenitors ($D^{lo}E^{lo}NF^{lo}$, $D^{lo}E^{hi}NF^{hi}$, and $D^{hi}E^{hi}NF^{lo}$) by our set of biophysical markers also exhibit high efficacy for in vivo osteogenic tissue regeneration. These results also show that a committed osteoprogenitor subpopulation ($D^{hi}E^{hi}NF^{lo}$) could be isolated consistently from the putative adult MSCs based on size alone (D^{hi}), using this high-throughput microfluidic device.

To further test this concept that biophysical markers are predictive of in vivo response, we examined the capacity of the different MSC subpopulations (as described above) to differentiate and repair myogenic tissue after injury in NOD/SCID mice. Although it is well established that the bone marrow-derived MSCs are precursors of tissues of mesenchymal origin including adipocytes, osteoblasts, and chondrocytes (45), others have reported previously that MSCs that exhibit mesenchymal trilineage differentiation in vitro can show markers of myogenic differentiation in vitro and in vivo (46, 47). This in vivo model for myogenic tissue repair has been reported previously (48). Briefly, 4 h after cardiotoxin injection into the gastrocnemius skeletal muscle, 30,000 MSCs were transplanted into the same region via localized injection to allow regeneration of the cardiotoxin-damaged skeletal muscle tissue. After a period of 20 d, the degree of muscle regeneration by MSCs was evaluated by histological examination. Fixed sections of the damaged muscles were stained with a human specific antibodies to detect human tissue engraftment and myogenic differentiation. Histological examinations revealed that, in damaged muscle tissue infused with both adult and fetal $D^{lo}E^{lo}NF^{hi}$ MSCs, extensive clusters of discrete green fluorescent spectrin-expressing myofiber-like tissues were present within the host muscle (Fig. 5 *D, i* and *ii*). In contrast, the committed osteoprogenitor subpopulations ($D^{lo}E^{hi}NF^{hi}$, $D^{lo}E^{lo}NF^{lo}$, and $D^{hi}E^{hi}NF^{lo}$) demonstrated limited engraftment and minimal myogenic differentiation.

Discussion

Here, we considered different biophysical markers of stem cells via methods that would enable robust identification and potential separation of committed progenitors from multipotent cells. Our multivariate analysis shows that there exists a minimal set of biophysical markers that can be used to determine MSC multipotency. Although large cell size (D^{hi}) consistently identifies committed osteoprogenitors in adult MSCs, multilineage potential (differentiation into adipo-, osteo-, chondro-, and myogenic lineages) is only observed if the cells are small, compliant, and exhibit large nuclear membrane fluctuations ($D^{lo}E^{lo}NF^{hi}$). The committed MSC subpopulations have a greater propensity to differentiate into osteoblasts and produce a greater extent of mineralization than the uncommitted MSCs described by the biophysical triplet, $D^{lo}E^{lo}NF^{hi}$. Interestingly, these committed subpopulations are not described uniquely by one biophysical triplet, but by multiple triplets that share in common the superthreshold magnitude of D and/or E and/or the subthreshold magnitude of NF; this multiplicity of biophysical descriptors for MSC-derived osteoprogenitors may reflect the multiplicity and extended duration of phenotypic differentiation pathways. A single device, the microfluidic spiral microchannel, is capable of high throughput isolation of osteoprogenitor cells (D^{hi} cells), which enables sorting of this subpopulation from marrow for applications such as bone regeneration. Additional future biophysical markers may include those that enable direct physical sorting of the solution suspended, multipotent $D^{lo}E^{lo}NF^{hi}$ cells. Furthermore, although beyond the scope of this study (*SI Appendix*), our approach could be extended to characterize the biophysical parameters of cells from clonal populations, which could shed further light on the mechanical ontogeny of MSCs after fewer population doublings in vitro.

Overall, our data support the hypothesis that $D^{lo}E^{lo}NF^{hi}$ MSCs are uncommitted, undifferentiated, clonogenic, and multipotent precursor subpopulations in culture-expanded cells derived from human bone marrow. Those biophysically distinct subpopulations may emerge on culture expansion (17), and the prevalence of such subpopulations can vary with donor or culture conditions. We believe that this multivariate approach and set of validated biophysical markers now offers the opportunity to identify and select the subpopulation of the multipotent mesenchymal stromal cells (or, alternatively, the osteoprogenitor cells) from heretofore mixed populations of culture-expanded, putative stem cell populations. This label-free method and analysis provide a necessary precursor to the robust study, engineering, and many therapeutic applications of these rare and valuable cells.

Methods

Cells analyzed herein were derived from bone marrow of five adult and five fetal donors, each obtained from commercial or consortia sources of low-passage putative MSCs (adult donors) or from established centrifugation and plastic-adherence subculture methods (fetal donors) (49). These cell populations from each donor source were thus considered to be mesenchymal stem cells according to existing, accepted methods. Briefly, for each of the 10 donor sources, the cell diameter was quantified, and physical sorting into cell size-specific subpopulations was achieved, by inertial microfluidic sorting of suspended cells; cell stiffness was quantified via atomic force microscopy-enabled nanoindentation of adhered living cells; and nuclear membrane fluctuations were quantified via customized image analysis of cells transfected to express fluorescent nuclear laminar proteins. Data discussed here correspond to passage 5 (population doubling ~10–12) for all donor sources for consistency, and mean ± SEM unless otherwise noted. See *SI Appendix* for detailed methods of biophysical characterization, in vitro and in vivo assays, and data analysis.

ACKNOWLEDGMENTS. We thank J. M. Maloney for valuable discussion of the manuscript and figures, V. H. W. Koh for assistance with microarray experiments, S. L. L. Ong for assistance with supporting graphics, M. S. K. Chong for feedback on in vitro and in vivo procedures, and A. A. S. Bhaghat for assistance with device fabrication. This research was supported by the National Research Foundation of Singapore through the Singapore MIT Alliance for Research and Technology's BioSystems and Micromechanics Interdisciplinary Research Group. W.C.L. also acknowledges the National University of Singapore Graduate School for Integrative Sciences and Engineering Program, and K.J.V.V., J.K.Y.C., and T.K. acknowledge the Singapore-MIT Alliance-3 graduate fellowship program. J.K.Y.C. received salary support from the National Medical Research Council, Singapore (NMRC/Clinician Scientist Award/012/2009).

1. Van Vliet KJ, Bao G, Suresh S (2003) The biomechanics toolbox: Experimental approaches for living cells and biomolecules. *Acta Mater* 51(19):5881–5905.
2. Suresh S (2007) Biomechanics and biophysics of cancer cells. *Acta Biomater* 3(4): 413–438.
3. Titushkin IA, Shin J, Cho M (2010) A new perspective for stem-cell mechanobiology: Biomechanical control of stem-cell behavior and fate. *Crit Rev Biomed Eng* 38(5): 393–433.
4. Ribeiro AJS, et al. (2012) Mechanical characterization of adult stem cells from bone marrow and perivascular niches. *J Biomech* 45(7):1280–1287.
5. Di Carlo D (2012) A mechanical biomarker of cell state in medicine. *J Lab Autom* 17(1): 32–42.
6. Guck J, et al. (2005) Optical deformability as an inherent cell marker for testing malignant transformation and metastatic competence. *Biophys J* 88(5):3689–3698.
7. Herricks T, Antia M, Rathod PK (2009) Deformability limits of Plasmodium falciparum-infected red blood cells. *Cell Microbiol* 11(9):1340–1353.
8. Maciaszek JL, Andemariam B, Lykotrafitis G (2011) Microelasticity of red blood cells in sickle cell disease. *J Strain Analysis Eng Design* 46(5):368–379.
9. Gossett DR, et al. (2012) Hydrodynamic stretching of single cells for large population mechanical phenotyping. *Proc Natl Acad Sci USA* 109(20):7630–7635.
10. Treiser MD, et al. (2010) Cytoskeleton-based forecasting of stem cell lineage fates. *Proc Natl Acad Sci USA* 107(2):610–615.
11. Gao FB, Raff M (1997) Cell size control and a cell-intrinsic maturation program in proliferating oligodendrocyte precursor cells. *J Cell Biol* 138(6):1367–1377.
12. Angello JC, Pendergrass WR, Norwood TH, Prothero J (1987) Proliferative potential of human fibroblasts: An inverse dependence on cell size. *J Cell Physiol* 132(1):125–130.
13. De Paiva CS, Pflugfelder SC, Li DQ (2006) Cell size correlates with phenotype and proliferative capacity in human corneal epithelial cells. *Stem Cells* 24(2):368–375.
14. González-Cruz RD, Fonseca VC, Darling EM (2012) Cellular mechanical properties reflect the differentiation potential of adipose-derived mesenchymal stem cells. *Proc Natl Acad Sci USA* 109(24):E1523–E1529.
15. Smith JR, Pochampally R, Perry A, Hsu SC, Prockop DJ (2004) Isolation of a highly clonogenic and multipotential subfraction of adult stem cells from bone marrow stroma. *Stem Cells* 22(5):823–831.
16. Colter DC, Sekiya I, Prockop DJ (2001) Identification of a subpopulation of rapidly self-renewing and multipotential adult stem cells in colonies of human marrow stromal cells. *Proc Natl Acad Sci USA* 98(14):7841–7845.
17. Whitfield MJ, Lee WC, Van Vliet KJ (2013) Onset of heterogeneity in culture-expanded bone marrow stromal cells. *Stem Cell Res (Amst)* 11(3):1365–1377.
18. McMurray RJ, et al. (2011) Nanoscale surfaces for the long-term maintenance of mesenchymal stem cell phenotype and multipotency. *Nat Mater* 10(8):637–644.
19. Pevsner-Fischer M, Levin S, Zipori D (2011) The origins of mesenchymal stromal cell heterogeneity. *Stem Cell Rev* 7(3):560–568.
20. Stein GS, Lian JB, Stein JL, Van Wijnen AJ, Montecino M (1996) Transcriptional control of osteoblast growth and differentiation. *Physiol Rev* 76(2):593–629.
21. Rosen ED, Spiegelman BM (2000) Molecular regulation of adipogenesis. *Annu Rev Cell Dev Biol* 16:145–171.
22. Zhao Q, Eberspaecher H, Lefebvre V, De Crombrugghe B (1997) Parallel expression of Sox9 and Col2a1 in cells undergoing chondrogenesis. *Dev Dyn* 209(4):377–386.
23. Engler AJ, Sen S, Sweeney HL, Discher DE (2006) Matrix elasticity directs stem cell lineage specification. *Cell* 126(4):677–689.
24. Dalby MJ, et al. (2007) The control of human mesenchymal cell differentiation using nanoscale symmetry and disorder. *Nat Mater* 6(12):997–1003.
25. Flaim CJ, Chien S, Bhatia SN (2005) An extracellular matrix microarray for probing cellular differentiation. *Nat Methods* 2(2):119–125.
26. Kolf CM, Cho E, Tuan RS (2007) Mesenchymal stromal cells. Biology of adult mesenchymal stem cells: Regulation of niche, self-renewal and differentiation. *Arthritis Res Ther* 9(1):204.
27. D'Ippolito G, et al. (2004) Marrow-isolated adult multilineage inducible (MIAMI) cells, a unique population of postnatal young and old human cells with extensive expansion and differentiation potential. *J Cell Sci* 117(Pt 14):2971–2981.
28. Van Vlasselaer P, Falla N, Snoeck H, Mathieu E (1994) Characterization and purification of osteogenic cells from murine bone marrow by two-color cell sorting using anti-Sca-1 monoclonal antibody and wheat germ agglutinin. *Blood* 84(3):753–763.
29. Sekiya I, et al. (2002) Expansion of human adult stem cells from bone marrow stroma: Conditions that maximize the yields of early progenitors and evaluate their quality. *Stem Cells* 20(6):530–541.
30. Lee RH, et al. (2009) The CD34-like protein PODXL and alpha6-integrin (CD49f) identify early progenitor MSCs with increased clonogenicity and migration to infarcted heart in mice. *Blood* 113(4):816–826.
31. Maloney JM, et al. (2010) Mesenchymal stem cell mechanics from the attached to the suspended state. *Biophys J* 99(8):2479–2487.
32. Jo CH, et al. (2008) Fetal mesenchymal stem cells derived from human umbilical cord sustain primitive characteristics during extensive expansion. *Cell Tissue Res* 334(3): 423–433.
33. Lee WC, et al. (2011) High-throughput cell cycle synchronization using inertial forces in spiral microchannels. *Lab Chip* 11(7):1359–1367.
34. Russell KC, et al. (2010) In vitro high-capacity assay to quantify the clonal heterogeneity in trilineage potential of mesenchymal stem cells reveals a complex hierarchy of lineage commitment. *Stem Cells* 28(4):788–798.
35. Efron B (1979) 1977 Rietz Lecture: Bootstrap methods: Another look at the jackknife. *Ann Stat* 7(1):1–26.
36. Chowdhury F, et al. (2010) Material properties of the cell dictate stress-induced spreading and differentiation in embryonic stem cells. *Nat Mater* 9(1):82–88.
37. Bhattacharya D, Talwar S, Mazumder A, Shivashankar GV (2009) Spatio-temporal plasticity in chromatin organization in mouse cell differentiation and during Drosophila embryogenesis. *Biophys J* 96(9):3832–3839.
38. Talwar S, Kumar A, Rao M, Menon GI, Shivashankar GV (2013) Correlated spatio-temporal fluctuations in chromatin compaction states characterize stem cells. *Biophys J* 104(3):553–564.
39. Meshorer E, et al. (2006) Hyperdynamic plasticity of chromatin proteins in pluripotent embryonic stem cells. *Dev Cell* 10(1):105–116.
40. Ullmann U, et al. (2007) Epithelial-mesenchymal transition process in human embryonic stem cells cultured in feeder-free conditions. *Mol Hum Reprod* 13(1):21–32.
41. Ribeiro AJS, Dahl KN (2010) The nucleus as a central structure in defining the mechanical properties of stem cells. *2010 Annual International Conference of the IEEE Engineering in Medicine and Biology Society*, Buenos Aires, Argentina (IEEE Engineering in Medicine and Biology Society, Piscataway, NJ), pp 831–834.
42. Williams SA, et al. (2011) USP1 deubiquitinates ID proteins to preserve a mesenchymal stem cell program in osteosarcoma. *Cell* 146(6):918–930.
43. Honczarenko M, et al. (2006) Human bone marrow stromal cells express a distinct set of biologically functional chemokine receptors. *Stem Cells* 24(4):1030–1041.
44. Zhang ZY, et al. (2009) Superior osteogenic capacity for bone tissue engineering of fetal compared with perinatal and adult mesenchymal stem cells. *Stem Cells* 27(1): 126–137.
45. Nombela-Arrieta C, Ritz J, Silberstein LE (2011) The elusive nature and function of mesenchymal stem cells. *Nat Rev Mol Cell Biol* 12(2):126–131.
46. Wakitani S, Saito T, Caplan AI (1995) Myogenic cells derived from rat bone marrow mesenchymal stem cells exposed to 5-azacytidine. *Muscle Nerve* 18(12):1417–1426.
47. Gonçalves MA, et al. (2006) Human mesenchymal stem cells ectopically expressing full-length dystrophin can complement Duchenne muscular dystrophy myotubes by cell fusion. *Hum Mol Genet* 15(2):213–221.
48. Crisan M, et al. (2008) A perivascular origin for mesenchymal stem cells in multiple human organs. *Cell Stem Cell* 3(3):301–313.
49. Chan J, et al. (2005) Human fetal mesenchymal stem cells as vehicles for gene delivery. *Stem Cells* 23(1):93–102.
50. Tarnowski M, et al. (2010) Optimization of genetic engineering and homologous recombination of collagen type I genes in rat bone marrow mesenchymal stem cells (MSC). *Cell Reprogram* 12(3):275–282.
51. Nassiri N, et al. (2011) Corneal endothelial cell changes after Ahmed valve and Molteno glaucoma implants. *Ophthalmic Surg Lasers Imaging* 42(5):394–399.